# A Role of Computational Modeling in Customization of Transcranial Direct Current Stimulation for Susceptible Populations

**10**

Dennis Truong, Preet Minhas, Albert Mokrejs, and Marom Bikson

## Introduction to Computational Models of Noninvasive Neuromodulation

Renewed interest in transcranial electrical stimulation has been accompanied by a general modernization of the technique including the use of computational models. This chapter introduces the rationale behind modeling transcranial direct current stimulation (tDCS) as well as the technical development and limitations of models currently in use. This chapter is intended to provide a broad introduction to both clinical researchers and engineers interested in translational work to develop and apply computational models of customized tDCS. Transcranial electrical stimulation is a promising tool in symptom management based on the growing evidence that delivery of current to specific brain regions can promote desirable plastic changes [1, 2]. However, stimulation should be applied using low intensity current in a manner that is safe and well tolerated. In complement to other brain stimulation approaches (Fig. 10.1), tDCS has been gaining considerable interest because it is well tolerated, and can be used as add-on therapy and has low maintenance costs [3].

In contrast to pharmacotherapy, noninvasive electrotherapy offers the potential for both anatomically specific brain activation and complete temporal control. Temporal control is achieved since electricity is delivered at the desired dose instantly and there is no electrical "residue" as the generated brain current disappears when stimulation is turned off. Spatial control is based on from rational selection of electrode number, shape, and position. As explained below, using computational models, tDCS can be customized and individualized to specific brain targets in ways not possible with other interventions in order to optimize a particular therapeutic or rehabilitative outcome. Specifically, the "dose" of electrotherapy (see Peterchev et al. [4] for definition) is readily adjustable by determining the location of electrodes (which determines spatial targeting) and selecting the stimulation waveform (which determines the nature and timing of neuromodulation). Indeed, a single programmable electrotherapy device can be simply configured to provide a diversity of dosages. Though this flexibly underpins the utility of neuromodulation, the myriad of potential dosages (stimulator settings and combinations of electrode placements) makes the optimal choice very difficult to readily ascertain. The essential issue in dose design is to relate each externally controlled dose with the associated brain regions targeted (and spared) by the resulting current flow—and hence the desired clinical outcome. Computational forward models aim to provide precisely these answers to the first part of this question (Fig. 10.2), and thus need to be leveraged in the rational design, interpretation, and optimization of neuromodulation.

The precise pattern of current flow through the brain is determined not only by the stimulation dose (e.g., the positions of the electrodes) but also by the underlying anatomy and tissue properties. In predicting brain current flow using computational models, it is thus important to precisely model both the stimulation itself and the relevant anatomy upon which it is delivered on an individual basis. The latter issue remains an area of ongoing technical development and is critical to establishing the clinical utility of these models. For example, cerebral spinal fluid (CSF) is highly conductive (a preferred "super highway" for current flow) such that details of CSF architecture profoundly shape current flow through adjacent brain regions (see later discussion).

D. Truong (✉) • P. Minhas
Department of Biomedical Engineering, The City College of New York, 160 Convent Avenue, ST-462, New York 10031, NY, USA
e-mail: dtruong01@ccny.cuny.edu

A. Mokrejs
Stuyvesant High School, Class 2016, 345 Chambers Street, New York, NY 10282, USA

M. Bikson
Neural Engineering Laboratory, Department of Biomedical Engineering, The City College of New York of CUNY, New York, NY, USA
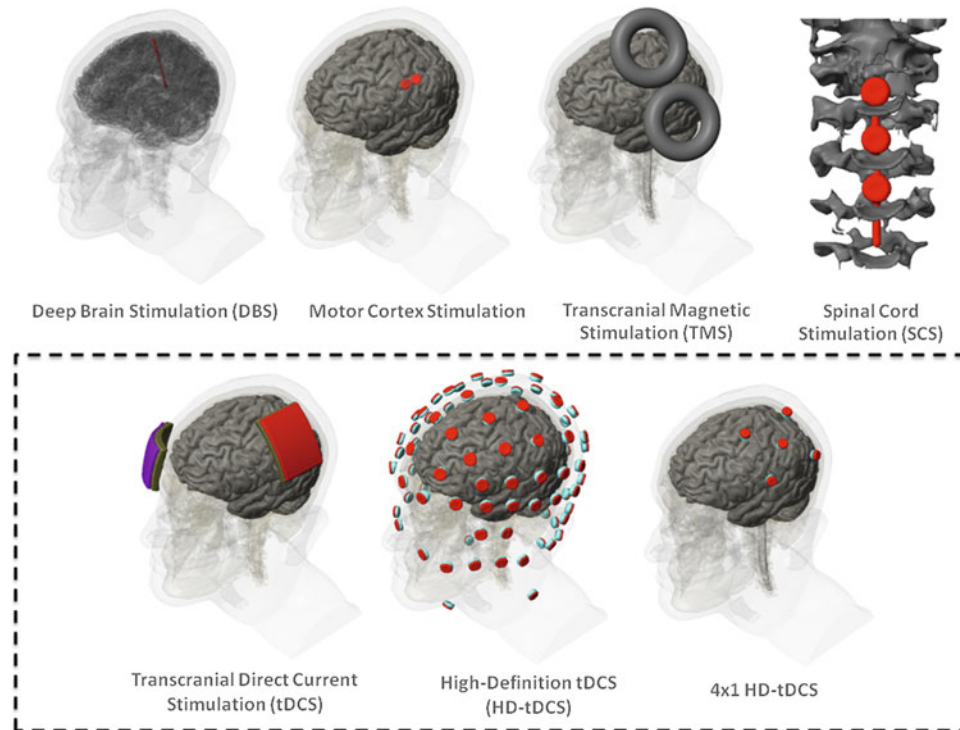
**Fig. 10.1** Comparable stimulation techniques: Deep Brain Stimulation, Motor Cortex Stimulation, Transcranial Magnetic Stimulation, and Spinal Cord Stimulation (*top row*); classic transcranial Direct Current Stimulation (tDCS) via sponge pads, optimized High Definition-tDCS (HD-tDCS), and $4 \times 1$ HD-tDCS (*bottom row*). Transcranial Direct Current Stimulation is an increasingly popular investigational form of brain stimulation, in part, due to its low cost, portability, usability, and safety. However, there are still many of unanswered questions. The number of potential stimulation doses is practically limitless. Stimulation can be varied by simply changing the electric current waveform and electrode shape, size, and position. These variations can thus be analyzed through computational modeling studies that have resulted in montages such as HD-tDCS and $4 \times 1$ HD-tDCS
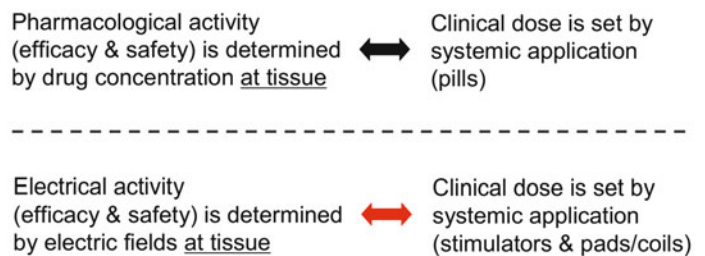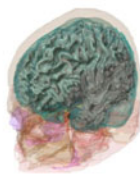


**Fig. 10.2** Role of computational models in rational electrotherapy: (*left*) Neuromodulation is a promising therapeutic modality as it affects the brain in a way not possible with other techniques with a high degree of individualized optimization. The goal of computational models is to assist clinicians in leveraging the power and flexibility of neuromodulation (*right*). Computational forward models are used to predict brain current flow during transcranial stimulation to guide clinical practice. As with pharmacotherapy, electrotherapy dose is controlled by the operator and leads a complex pattern of internal current flow that is described by the model. In this way, clinicians can apply computational models to determine which dose will activate (or avoid) brain regions of interest

Especially relevant for rehabilitative applications is the recognition that individual anatomical idiosyncrasies can result in significant distortions in current flow. This is particularly apparent when skull defects and brain lesions occur. The final section of this review highlights the nature and degree of distortions in brain current flow produced by defects and lesions, as well as dose considerations for susceptible populations such as children.

## Methods and Protocols in the Generation of Computational Forward Models of tDCS

During tDCS, current is generated in the brain. Because different electrode montages result in distinct brain current flow, researchers and clinicians can adjust the montage to target or avoid specific brain regions in an application specific manner. Though tDCS montage design often follows basic rules-of-thumb (e.g., increased/decreased excitability under the anode/cathode electrode), computational forward models of brain current flow provide more accurate insight into detailed current flow patterns and in some cases, can even challenge simplified electrode-placement assumptions [5–8]. For example, clinical studies are often designed by placing the anode electrode directly over the target region desired to be excited, while the cathode electrode is placed over a far removed region from the target to avoid unwanted reverse effects. This region could be the contralateral hemisphere or in some cases even extra cephalic locations like the neck, shoulder or the arm. Researchers have used smaller stimulation electrode sizes and bigger reference electrode sizes to offset the focality limitations of tDCS. With the increased recognized value of computational forward models in informing tDCS montage design and interpretation of results, there have been recent advances in modeling tools and a greater proliferation of publications [9–22].

Initial models of transcranial current flow assumed simplified geometries such as concentric spheres that could be solved analytically as well as numerically. Miranda et al. [15] was the first numerical modeling effort specifically looking at tDCS montages and intensities. In another spherical head paper, focality of cortical electrical fields was compared across various small electrode configurations and configurations proposed to achieve targeted modulation [10]. Wagner et al. [22] was the first computer-aided design (CAD) rendered head model where current density distributions were analyzed for various montages including healthy versus cortical stroke conditions. The more recent efforts have been mostly MRI derived. Oostendorp et al. [16] was the first to consider anisotropy in the skull and the white matter. Datta et al. [11] built the first high-resolution head model with gyri/sulci specificity. Using diffusion tensor imaging (DTI), Suh et al. [20] concluded that skull anisotropy causes a large shunting effect and may shift the stimulated areas. Fine resolution of gyri/sulci leads to current "hotspots" in the sulci, thereby reinforcing the need for high-resolution modeling [19]. Sadleir et al. [18] compared modeling predictions of frontal tDCS montages to clinical outcomes. Datta et al. [9] studied the effect of tDCS montages on TBI and skull defects. Parazzini et al. [17] was the first to analyze current flow patterns across subcortical structures. Dmochowski et al. [23] showed how a multi-electrode stimulation can be optimized for focality and intensity at the target.

Recent efforts have focused to build patient-specific models and compare modeling predictions to experimental outcomes. In considering new electrode montages, and especially in potentially vulnerable populations (e.g., in patients with skull damage or in children), forward models are the main tool used to relate the externally controllable dose parameters (e.g., electrode number, position, size, shape, current) with resulting brain current flow. While the specific software applications can vary across groups, in general, the approach and workflow for model generation follow a similar pattern (Fig. 10.3).

The steps for generating high-resolution (anatomically specific) forward models of noninvasive neuromodulation are adapted from extensive prior work on computational modeling. These involve: (1) Demarcation of individual tissue types (masks) from high-resolution anatomical data (e.g., magnetic resonance imaging slices obtained at 1 mm slice thickness) using a combination of automated and manual segmentation tools. Specifically, from the perspective of stimulating current flow, it is necessary to distinguish tissues by their resistivity. A majority of effort in the development and implementation of models has involved this step (see also next section) [18]. The number and precision of the individual masks obtained is pivotal for the generation of accurate 3D models in order to capture critical anatomical details that may influence current flow. (2) Modeling of the exact physical properties of the electrodes (e.g., shape and size) and precise placement within the segmented image data (i.e., along the skin mask outer surface). (3) Generation of accurate meshes (with a high-quality factor) from the tissue/electrode masks whilst preserving resolution of subject anatomical data. The generation of meshes is a process where each mask is divided into small contiguous "elements" which allow the current flow to then be numerically computed—hence the term "Finite Element Method" stimulations. (4) Resulting volumetric meshes are then imported into a commercial finite element (FE) solver. (5) At this step, resistivity is assigned to each mask (every element in each mask) and the boundary conditions are imposed including the current applied to the electrodes. (6) The standard Laplacian equation is solved using the appropriate numerical solver and tolerance settings. (7) Data is
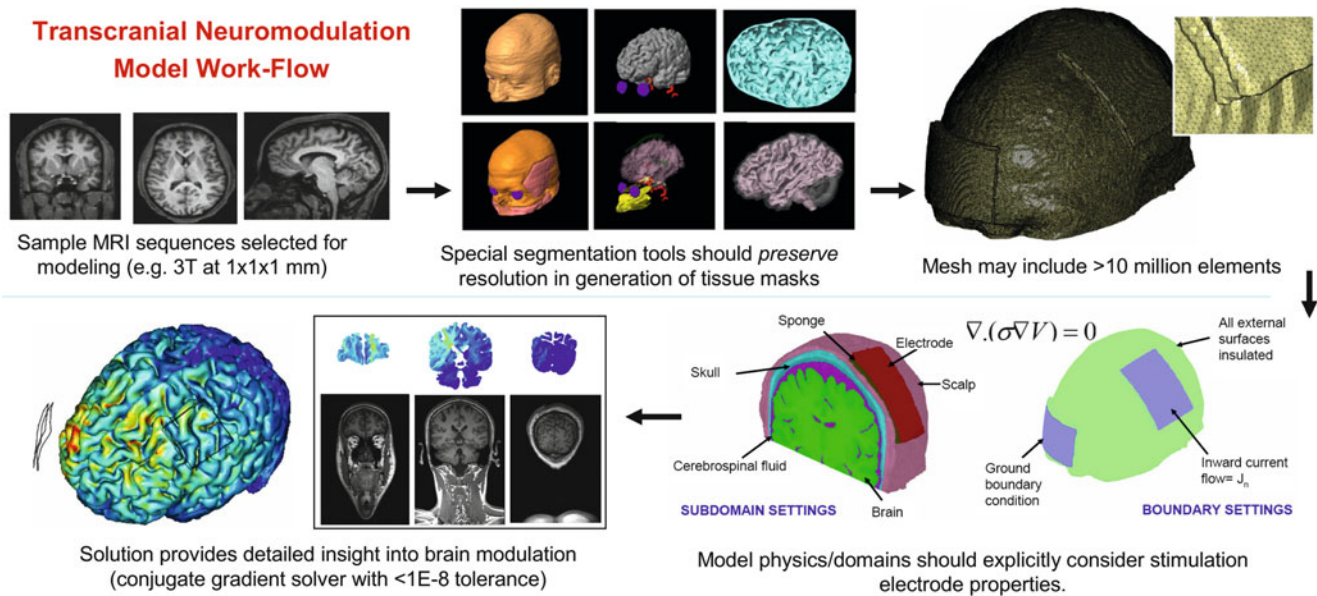
**Fig. 10.3** Imaging and computational work-flow for the generation of high-resolution individualized models: Though the specific processes and software packages will vary across technical groups and applications, in each case high-resolution modeling initiated with precise anatomical scans that allow demarcation of key tissues. Tissues with distinct resistivity are used to form "masks." These masks along with the representation of the physical electrodes are "meshed" to allow FEM calculations. The boundary conditions (generally simply reflecting how the electrodes are energized) and the governing equations (related to Ohms law) are well established. The reproduction of the stimulation dose and the underlying anatomy thus allow for the prediction of resulting brain current. These current flow patterns are represented in false-color map and analyzed through various post-processing tools

plotted as induced cortical electric field or current density maps (Fig. 10.3).

Though each of the above steps is required for high-resolution modeling, there remains technical expertise and hence variation in protocols across groups and publications [22]. These variations are relevant to clinical practice only in the sense that they change predictions in current flow that meaningfully effect dose decisions. The sources and impact of these variations is addressed in the next section.

Only a few studies have attempted to more directly link clinical outcomes and model predictions—and thus validate model utility. Clinical evaluation was combined with model predictions to investigate the effects of different montages in clinical conditions such as fibromyalgia [13]. Patient-specific models have been used to retrospectively analyze the therapeutic success of a given experimental stimulation montage [7] and compare model predictions with patterns of activation revealed by functional magnetic resonance imaging (fMRI) [12]. Postmortem "current flow imaging" was also used to validate general model prediction [24]. A focalized form of tDCS called $4 \times 1$ high-definition tDCS was developed through computational models and then validated in a clinical neurophysiology trial [25]. These example applications open the door for potentially customizing tDCS on a subject to subject basis within the clinical setting [26]. Table 10.1 summarizes the various tDCS montages explored in computational modeling studies.

For clinicians interested in using computational forward models to inform study design or interpretation several options are available. (1) A collaboration with a modeling group [21] or a company can allow for customized exploration of montage options; (2) referencing existing published reports or databases (Table 10.1) for comparable montages (with careful consideration of the role of individual variation and other caveats presented in the next section); (3) using a novel process where a desired brain region can be selected and the optimized electrode montage is proposed within a single step has been developed [23]; (4) a graphical user interface (GUI)-based program to stimulate arbitrary electrode montages in a spherical model is now available (www.neuralengr.com/spheres). This last solution illustrates an important trend: even as increasingly complex and resource expensive modeling tools are developed, parallel efforts to simplify and automate (high-throughput) model workflow are needed to facilitate clinical translation. If tDCS continues to emerge as an effective tool in clinical treatment and cognitive neuroscience, and concurrent modeling studies emphasize the need for rational (and in cases individualized) dose decisions, then it will become incumbent for tDCS researchers to understand the applications (and limitations) of computational forward models [27].

**Table 10.1** Synopsis of numerical tDCS computer models[a]

| Study | Masks | Electrode montage | Additional methods |
|---|---|---|---|
| Concentric sphere | | | |
| Miranda et al. (2006) [15] | 4 | 4 montages | |
| Datta et al. (2008) [10] | 4 | 6 montages | |
| Dmochowski et al. (2012) [23] Neuralengr.com/ spheres | 4 | Arbitrary, user specific, optimized montages | |
| CAD rendered | | | |
| Wagner (2007) [22] | 5 | Healthy and stroke models with varied montages | |
| MRI derived | | | |
| Oostendorp et al. (2008) [16] | 5 | C3–SO montage | Anisotropic conductivities for skull and white matter. Model derived from Wolters et al. (2006) [49] |
| Datta et al. (2009b) [11] | 4 | C3–SO and HD | High-resolution with gyrisulci topography |
| Suh et al. (2009) [8] | 5 | C3–SO montage using point source stimulation electrodes | Anisotropic conductivity for white matter |
| Datta et al. (2009b) [10] | 4 | Tissue temperature increases of C3–SO montage and HD montage | |
| Sadleir [10, 18] | 11 | F3–SO and F4–SO montage and comparison to reported clinical outcomes in literature | |
| Datta et al. (2010) [9] | 4 | Effect of skull defects and skull plates for C3–SO and 01–SO montages | |
| Bikson et al. (2010) [5] | 7 | C3–SO and C3-contralateral montages | Effect of "return electrode" position and size |
| Salvador et al. (2010) [19] | 5 | C3–SO montage | High-resolution gyrisulci model |
| Parazzini et al. (2011) [17] | 26 unique tissue types | Analysis of current flow through cortical, subcortical, and brain stem regions for C3–SO montage | Model derived from virtual family open source database |
| Mendonca et al. (2011) [13] | 8 | C3-extracephalic, SO-extracephalic and C3–SO montages | Correlation of clinical effects in a fibromyalgia study with model predictions |
| Halko et al. (2011) [12] | 7 | Oz–Cz montage | Patient-specific visual stroke model of a hemianopia patient undergoing tDCS. Correlation of high-resolution current flow model |
| Datta et al. (2011) [7] | 8 | Retrospective analysis comparing experimental outcome with model predictions. LFC-RS, LFC-contralateral mastoid, LFC-SO, RFC-LS | Patient-specific left hemisphere stroke model of a tDCS responder. |
| DaSilva et al. (2012) [6] | 15 | C3–SO montage analysis of current flow through subcortical structures | High-resolution individualized model |
| Turkeltaub et al. (2011) [21] | 8 | Analysis of left pTC and right pTC montage in dyslexia study | |
| Bonsai—model solution analyzer | 6–8 | Healthy and stroke model with varied montages | Online database of solved patient-specific head models. Overlaid views of 2D MRI scans and model solutions |
| Dmochowski et al. (2011) [23] | 6 | Healthy Head models with need-specific montages | Two distinct selections, focality based or intensity based |
| Wagner et al. (2011) [50] | 3 | Conventional tDCS montages | Inclusion of multicompartment/tissue layer anisotropy |
| Minhas et al. (2012) [48] | 2 | Conventional tDCS montages | Pediatric brain modeling |

[a]This table summarizes tDCS forward head models using FEM techniques. Head models have progressed from being spherical based to being MRI derived. The most recent ones have employed patient-specific models. The second, third, and fourth columns list number of tissue types, the montage used, and particular model specifics, respectively
C3, C4, F3, F4, O1, Oz, Cz correspond to 10/20 EEG system
*LFC* left frontal cortex, *LS* left shoulder, *pTC* posterior temporal cortex, *RFC* right frontal cortex, *RS* right shoulder, *SO* contralateral supra-orbital

## Pitfalls and Challenges in the Application and Interpretation of Computational Model Predictions

Computational models of tDCS range in complexity from concentric sphere models to high-resolution models based on individuals MRIs (as described above). The appropriate level of modeling detail depends on the clinical question being asked, as well as the available computational resources. Whereas simple geometries (e.g., spheres) may be solved analytically [28], realistic geometries employ numerical solvers, namely, Finite Element Methods (FEM). Regardless of complexity, all forward models share the goal of correctly predicting brain current flow during transcranial stimulation to guide clinical therapeutic delivery. Special effort has been recently directed towards increasing the precision of tDCS models. However, it is important to note that increased model complexity does not necessarily equate with greater accuracy or clinical value.

To meaningfully guide clinical utility, attempts to enhance model precision must rationally balance detail (i.e., complexity) and accuracy. (1) Beginning with high-resolution anatomical scans, the entire model workflow should preserve precision. Any human head model is limited by the precision and accuracy of tissue segmentation (i.e., "masks") and of the assigned conductivity values. One hallmark of precision is that the cortical surface used in the final FEM solver should capture realistic sulci and gyri anatomy. (2) Simultaneously, a priori knowledge of tissue anatomy and factors known to influence current flow should be applied to further refine segmentation. Particularly critical are discontinuities not present in nature that result from limited scan resolution; notably both unnatural perforations in planar tissues (e.g., ventricular architecture, discontinuities in CSF where brain contacts skull, misrepresented skull fissures,) and microstructures (e.g., incomplete or voxelized vessels) can produce significant deviations in predicted current flow. Moreover, because of the sensitivity of current flow to any conductivity boundary, increasingly detailed segmentation (e.g., globe of the eye and related structures, glands, and deeper midbrain structures) without reliable reported human conductivity values in literature (especially at static frequency) may also lead to errors. It is worth noting that the respective contribution of the automated/manual interventions also depends on: (a) sophistication of the particular database or automated algorithm employed since they are usually not optimized for forward transcranial modeling [7] and (b) the need for identification of anomalies in suspect populations like skull defects, lesions, shunts, etc. Thus, addition of complexity without proper parameterization can evidently decrease prediction accuracy. An improper balance between these factors can introduce distortions in predicted brain current flow.

Divergent modeling methods illustrate existing outstanding issues including: (1) detail in physically representing the stimulation electrodes and leads, including shape and material [8], and energy source boundary conditions; (2) differences between conductivity values derived from static resistivity measures and those extrapolated from 10 Hz data; (3) sufficient caudal head volume representation (such that the caudal boundary condition does not affect relevant model prediction), including potential use of synthetic volumes [7, 13]; (4) optimal imaging modalities/sequences to differentiate amongst tissue types; (5) appropriate incorporation of anisotropy (from DTI); (6) suitability of existing image segmentation algorithms (generally developed for other applications) [29]; (7) the degree and nature of manual correction; (8) the adequacy of the numerical solver (especially when making detailed predictions at tissue boundaries); (9) detail in segmenting true lesion borders [7] versus idealized defects; and (10) the need for parametric and interindividual analysis (see below). The optimization of the above issues remains open questions and inevitably reflects available resources (e.g., imaging, computational, anatomical expertise) and the specific clinical question addressed in each modeling effort. Even as computational and engineering groups continue developing more modeling sophistication, clinicians must be aware of the limitations in any modeling approach and the inevitability of technical methodology effecting the predictions made.

Having mentioned the importance of balancing increased complexity with clinical access to modeling, it is also important to emphasize a difference between the "value" of adding precision (complexity) as it is evaluated in engineering papers versus clinical translation. Increasingly detailed computational approaches have been proposed in recent years of varying anatomical and physiological details [16, 30, 17]. At the same time, computational models indicate subject specific variability in susceptibility to the same dose [26, 31, 32], indicating the value of individualized modeling, or at least modeling across a set of archetypes. Real clinical translational utility must therefore balance the value of increased sophistication with the cost associated with clinical scanning, computational time, and human resources/intervention (e.g., manual correction/pre and post-processing etc.). Thus the question is not if "different models will yield different predictions" (as must be posed in an engineering paper) but rather does increased complexity change model predictions in a way that is clinically meaningful—will complexity influence clinical decisions in study design. While this is a complex and application specific question, a first step toward systematizing value, across a myriad of

groups and efforts, is to develop a metric of change versus a simpler approach, and then applying a threshold based on perceived clinical value and added cost versus the simpler approach.

A priori, it is assumed that added detail/complexity will enhance model precision and, if done rationally, model accuracy [33]. Though an engineering group can devote extended resources and time to a "case" modeling study, the myriad of potential electrode combinations (dose) and variation across normal head [26] and pathological heads, means that in clinical trial design the particular models will likely now be solved (e.g., $4 \times 1$ over FP3 in a female head). Moreover, while "different models will yield different" predictions; practical dose decision is based on clinical study specific criterion "a meaningful clinical difference." Thus, two clinical applications of modeling are considered (1) Deciding across montages—namely, which montage is expected to achieve the optimal clinical outcomes in a given subject or on average across subjects; (2) Deciding on dose variation across subjects—namely, if and how to vary dose based on subject specific anatomy. It is further necessary to consider if the clinician is concerned with optimizing (a) intensity at the target (maximum current at the target regardless of overall brain current flow) or/and (b) focality at the target (intensity at the target relative to other brain regions); consideration of intensity of focality may lead to fundamentally different "best" dose [23]. In the first application, the clinician will compare different montages for their intensity and/or targeting of a brain region. Therefore, additional complexity and detail is only clinical meaningful if it results in a different selection of optimal montage based on either intensity or focality criterion.

Assuming accurate and precise representation of all tissue compartments (anatomy, resistivity, anisotropy) relevant to brain current flow, it is broadly assumed that using modern numerical solvers that the resulting prediction is independent of the numerical technique used. Our own experience across various commercial solvers confirms this implicit assumption when meshes are of sufficient detail—precise description in methods (use of publically available programs) and representation of resulting mesh density and quality (in figures or methods) as well as tests using various solvers provides explicit control for errors generated by the computation itself.

Literature regarding forward modeling—or more broadly the dissemination of modeling analysis to the clinical hands—introduces still further issues in regards to (1) interpretability, reproducibility, and accuracy (tissue masks) and (2) graphical representation of regions of influence (degree of "activation"). As there is no standard protocol for tissue imaging or segmentation, diversity in the nature of resulting tissue masks will invariably influence predicted current flow. As such, it is valuable to illustrate each 3D tissue mask in publication methods and/or classified serial sections. In regards to representation of relative activation, studies employ either maps of current density (unit of $A/m^2$) or electric field (unit of V/m). Because the two are related linearly by local tissue resistivity, when plotting activation in a region with uniform resistivity (for example the cortical surface), the spatial profile is identical. When plotting activation across tissues (e.g., coronal section), current density may be advantageous to illustrate overall brain current flow. However, the electric field in the brain is directly related to neuronal activation (e.g., for varied resistivity, the electric field, but not current density, provides sufficient information to predict activation). Despite best efforts, figure preparation invariably restricts tissue mask perspectives and comprehensive display of volumetric current flow, which can be supplemented with online data publication (http://www.neuralengr.com/bonsai).

When interpreting simulation predictions, it is important to recognize that the intensity of current flow in any specific brain region does not translate in any simple (linear) manner to the degree of brain activation or modulation (even when considering current direction). Moreover, recent neurophysiological studies indicate changes in "excitability" may not be monotonic with stimulation [34]. For example increasing stimulation amplitude or duration can invert the direction of modulation, as can the level of neuronal background activity [35]. However, to a first approximation, it seems reasonable to predict that regions with more current flow are more likely to be "effected" by stimulation while regions with little or no current flow will be spared the direct effects of stimulation. As the first step to understand mechanism of action of tDCS, a relationship between model predicted regional current flow and changes in functional activation was recently demonstrated [12]. The "quasi-uniform" assumption considers that if the electric field (current density) is uniform on the scale of a region/neuron of interest, then "excitability" may be modulated with local electric field intensity [36] (see discussion in [10] and [37]). Though efforts to develop suitable biophysical detailed models considering myriad of neurons with distinct positions and morphologies or "continuum" approximations [38] of modulation are pending, the current state-of-the-art requires (implicit) application of the "quasi-uniform" assumption.

Much of the theoretical and technical foundations for modeling brain stimulation were established through modeling studies on peripheral nerve stimulation ("Functional Electrical Stimulation," FES) and then Spinal Cord Stimulation (SCS) and Deep Brain Stimulation (DBS) (reviewed in[39–41]). In light of the challenges to tDCS modeling cited above, we note that FES and DBS use electrodes implanted in the body such that relatively small volume of brain is needed to be modeled, and with none of the complication associated with precisely representing

gross anatomy (e.g., skull, fat, or CSF). From the perspective of computational burden, the volume, number of masks, and mask complexity results in tDCS models with >5 million elements, compared to <200,000 elements for FES and DBS models. In addition, FES and DBS are suprathreshold allowing modeling studies to represent simply demarcated "regions of influence," inside which action potentials are triggered. tDCS affects large areas of superficial and deep brain structures (many types of cells and processes) and is subthreshold interacting with ongoing activity rather than driving action potentials, making it challenging to simply delineate "black-and-white" regions of influence.

Forward modeling studies and analysis are often published as "case reports" with predictions only on a single head [13, 17, 19, 21]. The suitability of single subject analysis reflects available (limited) resources and the clinical question being addressed. For a given electrode montage and stimulation dose, the sensitivity of global brain current to normal variation in anatomy (including across ages, gender) is unknown; however high-resolution modeling suggest gyri-specific dispersion of current flow, which could potentially account for individual variability. More generally, gross differences in tissue dimensions, notably skull thickness and CSF architecture, are expected to influence current flow. In some cases, modeling efforts specifically address the role of individual anatomical pathology, such as skull defects [9] or brain lesions [7]; it is precisely because these studies have shown the importance of specific defect/lesion details, that findings cannot be arbitrarily generalized. This in turn stresses the importance of individualized modeling as illustrated in the next section.

Though this section focused on the technical features of modeling, there is a broader concern in promoting effective collaboration between engineers and clinicians. For analogy, clinicians are generally aware of the challenges and pitfalls in post-processing and feature selection of fMRI data—and indeed, are thus intimately involved in data analysis rather than blindly relying on a technician. For computational "forward" models of neuromodulation, where results may inform study design and patient treatment, it is evidently as important to consider the uses and technical limitations of modeling approaches—and vigilance and skepticism on the part of clinicians will only enhance model rigor. Critically, for this reason, clinician/investigator experience and "judgment" supersedes all model predictions, even as these models form one important tool in dose design.

## Example Results of Computational Analysis in Susceptible Populations

### Case 1: Skull Defects

There is interest in the application of tDCS during rehabilitation of patients with brain lesions or skull defects (i.e., with or without skull plates); for example subjects with traumatic brain injury (TBI) or patients undergoing neurosurgery. As some of the neurological sequelae are presumably consequences of disrupted cortical activity following the traumatic event, the use of tDCS to deliver current to both damaged and compensatory regions in such circumstances can be a useful tool to reactivate and restore activity in essential neural networks associated with cognitive or motor processing. In addition, because of the reported antiseizure effects of tDCS [42], this technique might be useful for patients with refractory epilepsy who underwent surgery and have skull plates or decompressive craniectomy for trauma and cerebrovascular disease.

Despite rational incentives for investigation of tDCS in TBI or patients with other major neurological deficits and skull defects, one perceived limitation for the use of tDCS in these patients is the resulting modification of current flow by the skull defects and presence of surgical skull plates. Modeling studies can provide insight into how skull defects and skull plates would affect current flow through the brain and how to modify tDCS dose and/or electrode locations in such cases (Fig. 10.4). For example, a skull defect (craniotomy) that is filled with relatively highly conductive fluid or tissue represents a "shunt" pathway for current entering the brain but in a manner highly dependent on defect position relative to electrode montage. In such cases, the underlying cortex would then be exposed to a higher intensity of focused current flow. This in turn might be either beneficial in targeting the underlying brain region or hazardous if the increased current levels resulted in undesired neurophysiologic or pathological changes. Our modeling results confirm the notion that skull defects and skull plates can change the distribution of the current flow induced in cortical areas by tDCS. However, the details of current modulation depend entirely on the combination of electrode configuration and nature of the defect/plate, thus indicating the importance of individual analysis. Based on model predictions, application of tDCS without accounting for skull defects can lead to suboptimal and undesired brain current.
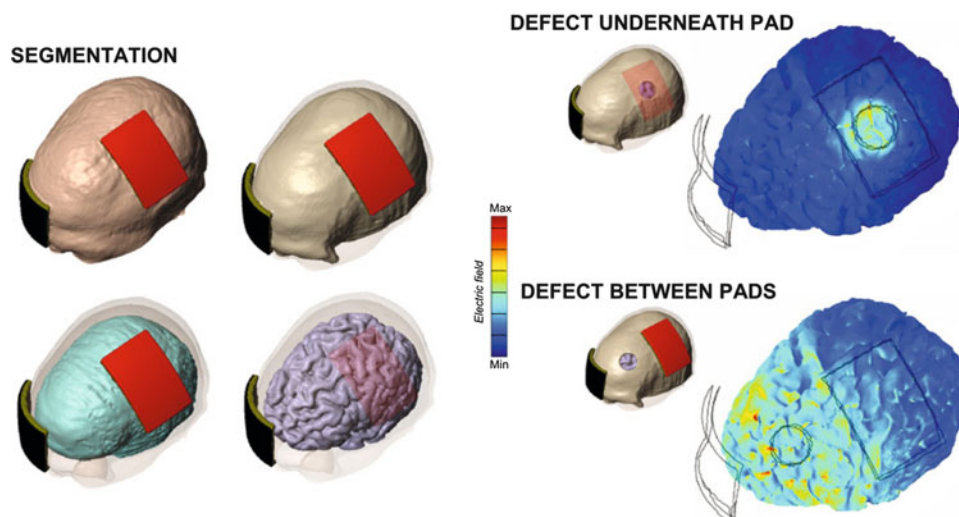
**Fig. 10.4** Computational model of current flow in subjects with skull defects/plates. A defect in skull tissue which is the most resistive tissue in the head would hypothetically effect current flow in the underlying brain regions. Furthermore, the exact location of the defect (under/between the stimulation pads) in combination with the "material" filling up the defect with the stimulation montage employed will influence induced current flow. Sample segmentation masks are shown on the *left*. A small defect under the anode pad (*top right*) leads to current flow in the cortex restricted to directly under the defect (avoiding the intermediate regions). A similar sized defect placed between the pads (*bottom right*) does not significantly alter current flow patterns in comparison with a healthy head with no defect. (Adapted from Datta et al. [9])

## Case 2: Brain Lesions (Stroke)

tDCS has been shown to modulate cognitive, linguistic, and motor performance in both healthy and neurologically impaired individuals with results supporting the feasibility of leveraging interactions between stimulation-induced neuromodulation and task execution [3]. As emphasized throughout this review, electrode montage (i.e., the position and size of electrodes) determines the resulting brain current flow and, as a result, neurophysiological effects. The ability to customize tDCS treatment through electrode montage provides clinical flexibility and the potential to individualize therapies. However, while numerous reports have been published in recent years demonstrating the effects of tDCS upon task performance, there remain fundamental questions about the optimal design of electrode configuration, especially around lesioned tissue [43]. Several modeling studies have predicted a profound influence of stroke related brain lesions on resulting brain current produced by tDCS [7, 12, 22].

Figure 10.5 illustrates an example of predicted current flow during tDCS from two subjects with a lesion due to stroke located with motor-frontal cortex (a) and occipital cortex (b) (adapted from [7] and [12]). Computational modeling suggests that current flow pattern during tDCS may be significantly altered by the presence of the lesion as compared to intact neurological tissue. Importantly, significant changes in the resulting cortical electric fields were observed not just around peri-lesional regions but also within wider cortical regions beyond the location of the electrodes. In a sense, the lesion itself acts as a "virtual" electrode modulating the overall current flow pattern [7].

## Case 3: Pediatric Populations

There is increasing interest in the use of neuromodulation in pediatric populations for a range of indications including rehabilitation, cognitive performance, and epilepsy treatment [44–46]. However, a rational protocol/guideline for the use of tDCS on children has not been formally established. Previous modeling studies have shown that current flow behavior is dependent on *both* the tDCS dose (montage and current intensity) and the underlying brain anatomy. Because of anatomical differences (skull thickness, CSF volume, and gray/white matter volume) between a growing child and an adult it is expected that the resulting brain current intensity in a child would be different as compared to that in an adult. Evidently, it would not be prudent to adjust stimulation dose for children through an arbitrary rule of thumb (e.g., reduce electrode size and current intensity by the ratio of head diameter). Again, computational forward models provide direct insight into the relation between external tDCS dose and resulting brain current and thus can inform dose design in children. Figure 10.6 shows an example of a model of tDCS in a 12-year old compared to that of a standard adult model. Both the peak and spatial distribution of current in the

**Fig. 10.5** Computational models predict current flow during tDCS in subjects with lesions. Brain lesions, as occur during stroke, are considered to be largely cannibalized and replaced by CSF, which is significantly more conductive than brain. For this reason, brain current flow during tDCS is expected to be altered. (**a**) Patient-specific left hemisphere stroke model. Two stimulation montages are illustrated, a conventional sponge montage (*top right*) and a high-definition montage (*bottom right*). (**b**) Patient-specific visual stroke model. Segmentation masks (*left*) and induced current flow using the experimental montage (*right*). (Adapted from Datta et al. [7] and Halko et al. [12])
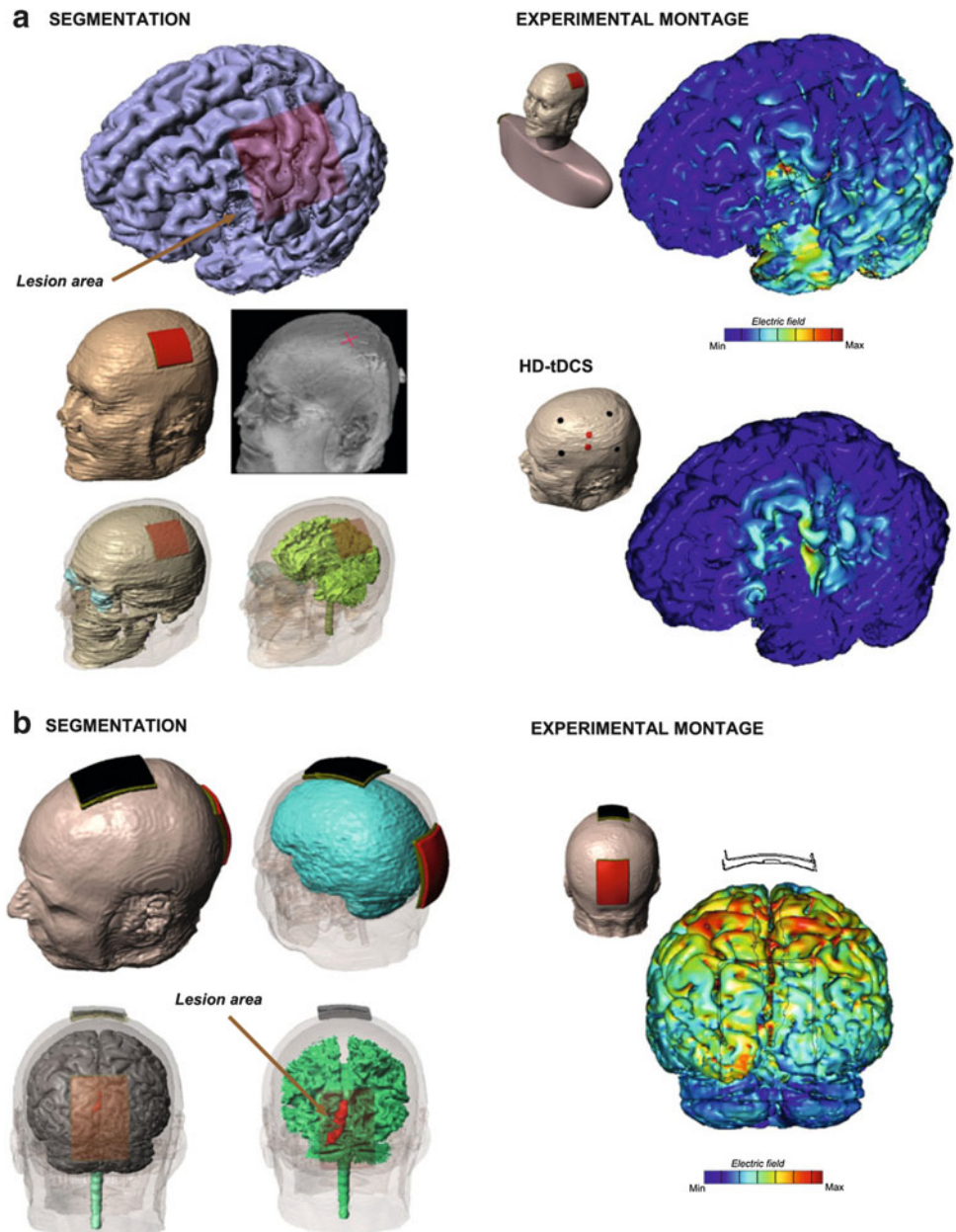


brain is altered compared to the typical adult case. In fact, for this particular case, the peak electric fields, at a given intensity, were nearly double in the 12-year-old as compared to the adult. Though questions remain about the impact of gross anatomical differences in altering generated brain current flow during neuromodulation, computational "forward" models provide direct insight into this question, and may ultimately be used to rationally adjust stimulation dose.

## Case 4: Obesity

The wide range of uses for tDCS makes it applicable to a diverse population that can include obese subjects.

Montages that have been evaluated for pain, depression, or appetite suppression have been modeled in average adults, but unique challenges exist in the obese model (Fig. 10.7). The additional subcutaneous fat present in the obese model warranted an additional layer of complexity beyond the commonly used five tissue model (skin, skull, CSF, gray matter, white matter). Including fat in the model of a super-obese subject led to an increase in cortical electric field magnitude of approximately 60 % compared to the model without fat (Fig. 10.7, a.1–a.3). A shift was also seen in the spatial distribution of the cortical electric field, most noticeable on the orbitofrontal cortex.

To gain an intuition for how subcutaneous fat influences cortical electric field and current density, additional models
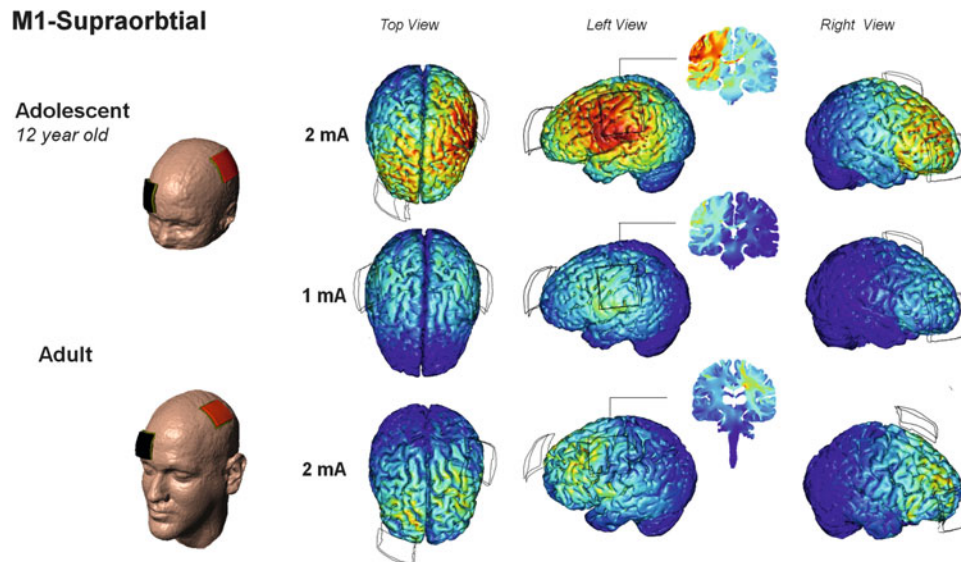
**Fig. 10.6** Individualized head model of a two adolescents as compared to an adult: Induced current flow for motor cortex tDCS at different intensities 1 mA of stimulation in the adolescent is comparable to 2 mA of stimulation in an adult
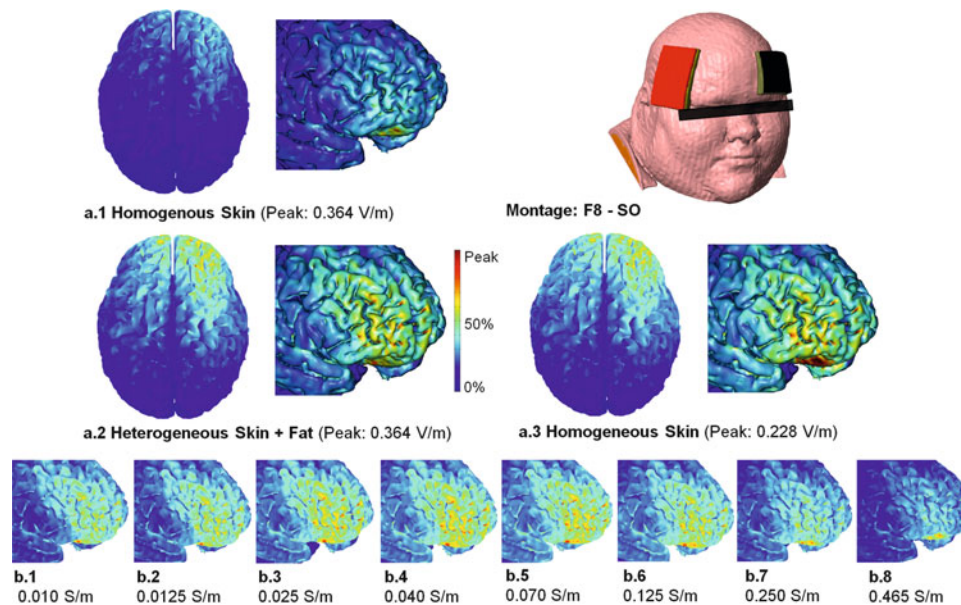


**Fig. 10.7** Predicted cortical electric field during inferior prefrontal cortex stimulation via $5'' \times 7''$ pads. Two conditions, homogenous skin (**a**.1) and heterogeneous skin (**a**.2), are contrasted on the same scale (0.364 V/m/mA peak). The homogeneous skin condition is displayed (**a**.3) at a lowered scale (0.228 V/m/mA peak) to compare the spatial distribution to the heterogeneous condition (**a**.2). The effect due to a range of varying fat conductivities (**b**.1–8) is compared on a fixed scale (0.364 V/m/mA peak). The conductivity of fat (0.025 S/m) is within an "optimum" range of influence that causes an increase in peak cortical electric field when included (Adapted from [47])

examined a range of conductivity values from the conductivity of skull (0.010 S/m, Fig. 10.7 b.1) to the conductivity of skin (0.465 S/m, Fig. 10.7 b.8). Coincidentally, the conductivity commonly used for fat (0.025 S/m, Fig. 10.7 b.4) was in the range that causes a peak increase in cortical electric field magnitude. It was postulated that more current was blocked by subcutaneous fat at an extremely low conductivity (b.1), while more current was redirected at an extremely high conductivity. This, in effect, led to an "optimum" range of influence where the conductivity of fat is believed to reside.

Ultimately, the need to precisely parameterize models rests hand-in-hand with the intended use of the model. From an engineering perspective, the increased complexity

**Fig. 10.8** Predicted electric field peak from a model relative to the factor of scaling to electrode sponge size (**a**). The effect is mapped on a linear scale, which shows a visible curve of exponential decrease (**b**). The effect of scaling the resistance of skin layers at a fixed ration is also graphed from the same model and relative to electric field peak. The curve formed by the data points is of exponential decrease as well (**c**)
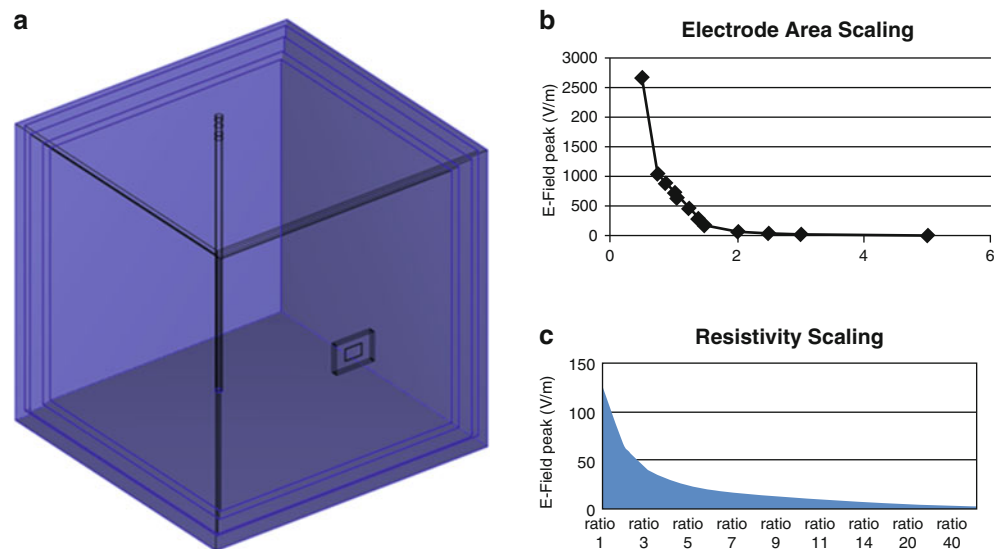
of this model caused a noteworthy change within the subject modeled, but this change would not be clinically noteworthy if stimulation dose does not change from subject to subject. This clinical analysis requires an additional comparison between subjects and consideration of the wide variation already inherent in "typical" subjects [26]. What can be concluded, however, is that a comparison between models would require consistent parameterization of subcutaneous fat.

## Case 5: Skin Properties

Computational models can vary in detail to accommodate various amounts of layers and other features such as blood vessels or sweat pores. Skin in particular can be rendered in varying levels of detail due its natural division into different layers, although even personalized models often simply make it a single layer.

In the model used to create Fig. 10.8, skin is portrayed as two layers one constituting the dermis and the other the epidermis and there are five layers in total. The model was solved for Electric-Field Peak for two separate characteristics, the ratio between tissue resistivity (The ratios between the various tissues being kept fixed, but scaled to see how the scale affected Electric Field), and for the scale of the area of the electrode sponges (The electrodes keeping their dimensional ratios but having their surface area scaled to determine the relationship between surface area and Electric field). Both models showed visible trends which are displayed in the graphs of Fig. 10.8 respectively.

While MRI-derived models are the standard for subject specific modeling, generalized models can be used to deduce trends applicable across populations. This is especially beneficial in cases where personalized cranial models are not

necessary or not available. These simplified models allow for the observation and prediction of data in more complex personalized models.

These cases demonstrate the potentially profound influence of lesions and skull defects on resulting current flow, as well as the need to customize tDCS montages to gross individual head dimensions. If tDCS continues to become a viable option for treatment in cases such as chronic stroke, the consideration of tDCS-induced current flow through the brain is of fundamental importance for the identification of candidates, optimization of electrotherapies for specific brain targets, and interpretation of patient-specific results. Thus, the ability and value of individualized tDCS therapy must be leveraged. Whereas, tDCS electrode montages are commonly designed using "gross" intuitive general rules (*eg*, anode electrode positioned "over" the target region), the value of applying predictive modeling as one tool in the rational design of safe and effective electrotherapies is becoming increasingly recognized.

Electrode montage (i.e., the position and size of electrodes) determines the resulting brain current flow and, as a result, neurophysiological effects. The ability to customize tDCS treatment through electrode montage provides clinical flexibility and the potential to individualize therapies [5, 7, 13]. However, while numerous reports have been published in recent years demonstrating the effects of tDCS upon task performance, there remain fundamental questions about the optimal design of electrode configurations with computational "forward" models playing a pivotal role.

### Conclusion

While numerous published reports have demonstrated the beneficial effects of tDCS upon task performance, fundamental questions remain regarding the optimal electrode

configuration on the scalp. Moreover, it is expected that individual anatomical differences in the extreme case manifest as skull defects and lesioned brain tissue which consequently will influence current flow and should therefore be considered (and perhaps leveraged) in the optimization of neuromodulation therapies. Heterogeneity in clinical responses may result from many sources, but the role of altered bran current flow due to both normal and pathological is tractable using computational "forward" models, which can then be leveraged to individualize therapy. Increasing emphasis on high-resolution (subject specific) modeling, provides motivation for individual analysis leading to optimized and customized therapy.

## References

1. Ardolino G, Bossi B, Barbieri S, Priori A. Non-synaptic mechanisms underlie the after-effects of cathodal transcutaneous direct current stimulton of the human brain. J Physiol. 2005;568:653–63.
2. Zentner J. Noninvasive motor evoked potential monitoring during neurosurgical operations on the spinal cord. Neurosurgery. 1989;24:709–12.
3. Brunoni AR, Nitsche MA, Bolognini N, Bikson M, Wagner T, Merabet L, Edwards DJ, et al. Clinical research with transcranial direct current stimulation (tDCS): challenges and future directions. Brain Stimul. 2012;5(3):175–95.
4. Peterchev A, Wagner T, Miranda P, Nitsche M, Paulus W, Lisanby S, et al. Fundamentals of transcranial electric and magnetic stimulation dose: definition, selection, and reporting practices. Brain Stimul. 2012;5:435–53.
5. Bikson M, Datta A, Rahman A, Scaturro J. Electrode montages for tDCS and weak transcranial electrical stimulation: role of "return" electrode's position and size. Clin Neurophysiol. 2010;121:1976–8.
6. DaSilva AF, Mendonca ME, Zaghi S, Lopes M, Dossantos MF, Spierings EL, et al. tDCS-induced analgesia and electrical fields in pain-related neural networks in chronic migraine. Headache. 2012;52:1283–95.
7. Datta A, Baker J, Bikson M, Fridriksson J. Individualized model predicts brain current flow during transcranial direct-current stimulation treatment in responsive stroke patient. Brain Stimul. 2011;4:169–74.
8. Datta A, Bansal V, Diaz J, Patel J, Reato D, Bikson M. Gyri-precise head model of transcranial direct current stimulation: improved spatial focality using a ring electrode versus conventional rectangular pad. Brain Stimul. 2009;2:201–7.
9. Datta A, Bikson M, Fregni F. Transcranial direct current stimulation in patients with skull defects and skull plates: high-resolution computational FEM study of factors altering cortical current flow. Neuroimage. 2010;52:1268–78.
10. Datta A, Elwassif M, Battaglia F, Bikson M. Transcranial current stimulation focality using disc and ring electrode configurations: FEM analysis. J Neural Eng. 2008;5:163–74.
11. Datta A, Elwassif M, Bikson M. Bio-heat transfer model of transcranial DC stimulation: comparison of conventional pad versus ring electrode. Conf Proc IEEE Eng Med Biol Soc. 2009;2009:670–3.
12. Halko MA, Datta A, Plow EB, Scaturro J, Bikson M, Merabet LB. Neuroplastic changes following rehabilitative training correlate with regional electrical field induced with tDCS. Neuroimage. 2011;57:885–91.
13. Mendonca ME, Santana MB, Baptista AF, Datta A, Bikson M, Fregni F, et al. Transcranial DC stimulation in fibromyalgia: optimized cortical target supported by high-resolution computational models. J Pain. 2011;12:610–7.
14. Miranda PC, Faria P, Hallett M. What does the ratio of injected current to electrode area tell us about current density in the brain during tDCS? Clin Neurophysiol. 2009;120:1183–7.
15. Miranda PC, Lomarev M, Hallett M. Modeling the current distribution during transcranial direct current stimulation. Clin Neurophysiol. 2006;117:1623–9.
16. Oostendorp TF, Hengeveld YA, Wolters CH, Stinstra J, van Elswijk G, Stegeman DF. Modeling transcranial DC stimulation. Conf Proc IEEE Eng Med Biol Soc. 2008;2008:4226–9.
17. Parazzini M, Fiocchi S, Rossi E, Paglialonga A, Ravazzani P. Transcranial direct current stimulation: estimation of the electric field and of the current density in an anatomical head model. IEEE Trans Biomed Eng. 2011;58:1773–80.
18. Sadleir RJ, Vannorsdall TD, Schretlen DJ, Gordon B. Transcranial direct current stimulation (tDCS) in a realistic head model. Neuroimage. 2010;51:1310–8.
19. Salvador R, Mekonnen A, Ruffini G, Miranda PC. Modeling the electric field induced in a high resolution head model during transcranial current stimulation. Conf Proc IEEE Eng Med Biol Soc. 2010;2010:2073–6.
20. Suh HS, Kim SH, Lee WH, Kim TS. Realistic simulation of transcranial direct current stimulation via 3-d high resolution finite element analysis: effect of tissue anisotropy. Conf Proc IEEE Eng Med Biol Soc. 2009;2009:638–41.
21. Turkeltaub PE, Benson J, Hamilton RH, Datta A, Bikson M, Coslett HB. Left lateralizing transcranial direct current stimulation improves reading efficiency. Brain Stimul. 2012;5:201–7.
22. Wagner T, Fregni F, Fecteau S, Grodzinsky A, Zahn M, Pascual-Leone A. Transcranial direct current stimulation:a computer-based human model study. Neuroimage. 2007;35:1113–24.
23. Dmochowski JP, Datta A, Bikson M, Su Y, Parra LC. Optimized multi-electrode stimulation increases focality and intensity at target. J Neural Eng. 2011;8:046011.
24. Antal A, Bikson M, Datta A, Lafon B, Dechent P, Parra LC, et al. Imaging artifacts induced by electrical stimulation during conventional fMRI of the brain. NeuroImage. 2014;85:1040–7.
25. Kuo HI, Bikson M, Datta A, Minhas P, Paulus W, Kuo MF, et al. Comparing cortical plasticity induced by conventional and high-definition 4 x 1 ring tDCS: A neurophysiological study. Brain Stimul. 2013;6:644–8.
26. Datta A, Truong D, Minhas P, Parra LC, Bikson M. Inter-individual variation during transcranial direct current stimulation and normalization of dose using MRI-derived computational models. Front Psychiatry. 2012;3:91.
27. Borckardt JJ, Bikson M, Frohman H, Reeves ST, Datta A, Bansal V, et al. A pilot study of the tolerability, safety and effects of high-definition transcranial direct current stimulation (HD-tDCS) on pain perception. J Pain. 2012;13:112–20.
28. Rush S, Driscoll DA. Current distribution in the brain from surface electrodes. Anesth Analg. 1968;47:717–23.
29. Smith SM. Fast robust automated brain extraction. Hum Brain Mapp. 2002;17(3):143–55.
30. Parazzini M, Fiocchi S, Ravazzani P. Electric field and current density distribution in an anatomical head model during transcranial direct current stimulation for tinnitus treatment. Bioelectromagnetics. 2012;33:476–87.
31. Shahid S, Wen P, Ahfock T. Numerical investigation of white matter anisotropic conductivity in defining current distribution under tDCS. Comput Methods Programs Biomed. 2013;109 (1):48–64.

32. Bikson M, Datta A. Guidelines for precise and accurate computational models of tDCS. Brain Stimul. 2012;5(3):430–1. doi:10.1016/j.brs.2011.06.001.

33. Bikson M, Rahman A, Datta A. Computational models of transcranial direct current stimulation. Clin EEG Neurosci. 2012;43(3):176–83.

34. Lindenberg R, Zhu LL, Schlaug G. Combined central and peripheral stimulation to facilitate motor recovery after stroke: the effect of number of sessions on outcome. Neurorehabil Neural Repair. 2012;26(5):479–83.

35. Nitsche MA, Paulus W. Sustained excitability elevations induced by transcranial DC motor cortex stimulation in humans. Neurology. 2001;57:1899–901.

36. Bikson M, Inoue M, Akiyama H, Deans JK, Fox JE, Miyakawa H, et al. Effects of uniform extracellular DC electric fields on excitability in rat hippocampal slices in vitro. J Physiol. 2004;557:175–90.

37. Miranda PC, Correia L, Salvador R, Basser PJ. The role of tissue heterogeneity in neural stimulation by applied electric fields. Conf Proc IEEE Eng Med Biol Soc. 2007;2007:1715–8.

38. Joucla S, Yvert B. The "mirror" estimate: an intuitive predictor of membrane polarization during extracellular stimulation. Biophys J. 2009;96(9):3495–508.

39. McIntyre CC, Miocinovic S, Butson CR. Computational analysis of deep brain stimulation. Expert Rev Med Devices. 2007;4:615–22.

40. Holsheimer J. Computer modelling of spinal cord stimulation and its contribution to therapeutic efficacy. Spinal Cord. 1998;36:531–40.

41. Rattay F. Analysis of models for external stimulation of axons. IEEE Trans Biomed Eng. 1986;33:974–7.

42. Fregni F, Thome-Souza S, Nitsche MA, Freedman SD, Valente KD, Pascual-Leone A. A controlled clinical trial of cathodal DC polarization in patients with refractory epilepsy. Epilepsia. 2006;47:335–42.

43. Fridriksson J. Measuring and inducing brain plasticity in chronic aphasia. J Commun Disord. 2011;44(5):557–63.

44. Mattai A, Miller R, Weisinger B, Greenstein D, Bakalar J, Tossell J, et al. Tolerability of transcranial direct current stimulation in childhood-onset schizophrenia. Brain Stimul. 2011;4:275–80.

45. Schneider HD, Hopp JP. The use of the Bilingual Aphasia Test for assessment and transcranial direct current stimulation to modulate language acquisition in minimally verbal children with autism. Clin Linguist Phon. 2011;25(6–7):640–54.

46. Varga ET, Terney D, Atkins MD, Nikanorova M, Jeppesen DS, Uldall P, et al. Transcranial direct current stimulation in refractory continuous spikes and waves during slow sleep: a controlled study. Epilepsy Res. 2011;97:142–5.

47. Truong DQ, Magerowski G, Pascual-Leone A, Alonso-Alonso M, Bikson M. Finite element study of skin and fat delineation in an obese subject for transcranial direct current stimulation. Conf Proc IEEE Eng Med Biol Soc. 2012;2012:6587–90.

48. Minhas P, Bikson M, Woods AJ, Rosen AR, Kessler SK. Transcranial direct current stimulation in pediatric brain: a computational modeling study. Conf Proc IEEE Eng Med Biol Soc. 2012;2012:859–62.

49. Wolters CH, Anwander A, Tricoche X, Weinstein D, Koch MA, MacLeod RS. Influence of tissue conductivity anisotropy on EEG/MEG field and return current computation in a realistic head model: a simulation and visualization study using high-resolution finite element modeling. Neuroimage. 2006;30(3):813–26.

50. Wagner TA, Eden UT. Systems and methods for stimulating and monitoring biological tissue. U.S. Patent Application 13/162,047, filed June 16, 2011.